1521-0103/370/3/671–681$35.00
THE JOURNAL OF PHARMACOLOGY AND EXPERIMENTAL THERAPEUTICS

https://doi.org/10.1124/jpet.118.256230
J Pharmacol Exp Ther 370:671–681, September 2019

The Journal of PHARMACOLOGY And Experimental Therapeutics

Special Section on Drug Delivery Technologies—Minireview

Translating Nanomedicine to Comparative Oncology—the Case for Combining Zinc Oxide Nanomaterials with Nucleic Acid Therapeutic and Protein Delivery for Treating Metastatic Cancer

R.K. DeLong, Yi-Hsien Cheng, Paige Pearson, Zhoumeng Lin, Calli Coffee, Elza Neelima Mathew, Amanda Hoffman, Raelene M. Wouda, and Mary Lynn Higginbotham

Department of Anatomy and Physiology, Nanotechnology Innovation Center (R.K.D., P.P., E.N.M., A.H.), Department of Anatomy and Physiology, Institute for Computational Comparative Medicine (Y.-H.C., Z.L.), and Department of Clinical Sciences (C.C., R.M.W., M.L.H.), College of Veterinary Medicine, Kansas State University, Manhattan, Kansas

Received January 3, 2019; accepted April 4, 2019

ABSTRACT

The unique anticancer, biochemical, and immunologic properties of nanomaterials are becoming a new tool in biomedical research. Their translation into the clinic promises a new wave of targeted therapies. One nanomaterial of particular interest are zinc oxide (ZnO) nanoparticles (NPs), which has distinct mechanisms of anticancer activity including unique surface, induction of reactive oxygen species, lipid oxidation, pH, and also ionic gradients within cancer cells and the tumor microenvironment. It is recognized that ZnO NPs can serve as a direct enzyme inhibitor. Significantly, ZnO NPs inhibit extracellular signal–regulated kinase (ERK) and protein kinase B (AKT) associated with melanoma progression, drug resistance, and metastasis. Indeed, direct intratumoral injection of ZnO NPs or a complex of ZnO with RNA significantly suppresses ERK and AKT phosphorylation. These data suggest ZnO NPs and their complexes or conjugates with nucleic acid therapeutic or anticancer protein may represent a potential new strategy for the treatment of metastatic melanoma, and potentially other cancers. This review focuses on the anticancer mechanisms of ZnO NPs and what is currently known about its biochemical effects on melanoma, biologic activity, and pharmacokinetics in rodents and its potential for translation into large animal, spontaneously developing models of melanoma and other cancers, which represent models of comparative oncology.

Introduction

Cancer and Nanomedicine. Based on recent World Health Organization estimates, cancer is responsible for nearly one in six deaths and has a significant and increasing worldwide economic impact (http://www.who.int/news-room/fact-sheets/detail/cancer). Traditional treatment methods including surgery, radiation, and chemotherapy have limited success in controlling metastatic disease. While better therapies are needed for many, if not most, metastatic cancers, the incidence and associated death rate of melanoma (cancer of the skin) continues to climb despite the availability of targeted small molecule inhibitors and newer immunotherapies (Robert et al., 2015; Weber et al., 2017; Sakamuri et al., 2018). Thus, additional treatment options are urgently needed for metastatic melanoma.

Importantly in the last decade, nanomedicine has emerged with transformative power and its cancer treatment potential is just beginning to be realized (Li et al., 2015; https://www.mccormick.northwestern.edu/news/articles/2017/05/first-spherical-nucleic-acid-drug-injected-into-humans-targets-brain-cancer.html; Tran et al., 2017; Liu et al., 2018). While chemotherapy drugs act systemically, once bound to a tiny nanoparticle (NP) with an inversely proportionate large surface area, the drug concentration—and, hence, effective dose delivered—is substantially increased. However, in the absence of a targeting agent such as an antibody conjugated to the NP, NPs indiscriminately bind or enter cancerous and normal cells, which may result in toxicity and suboptimal tumor targeting, much the same as conventional

This work was supported in part by the National Institutes of Health National Institute of Biomedical Imaging and Bioengineering [Award R03EB025566] (to R.K.D., Y.-H.Z., and Z.L.).
The content of this paper is solely the responsibility of the authors and does not necessarily represent the official views of the National Institutes of Health.
https://doi.org/10.1124/jpet.118.256230.

ABBREVIATIONS: ACP, anticancer protein; AKT, protein kinase B; Au, gold; CSNP, core-shell nanoparticle; ERK, extracellular signal–regulated kinase; Fe_3O_4, iron oxide; NAT, nucleic acid therapeutic; NP, nanoparticle; PBPK, physiologically-based pharmacokinetics; PEG, polyethylene glycol; PK, pharmacokinetics; poly I:C, polyinosinic:polycytidylic acid; RBD, Ras-binding domain; ROS, reactive oxygen species; ZnO, zinc oxide.

chemotherapy agents. There are two mechanisms by which NP targeting of tumor cells may be achieved. Passive targeting of NPs occurs because of the small size of the NPs and their ability to carry drug payload into the tumor microenvironment due to its microvascularization, whereas active targeting of NPs occurs due to functionalization of the surface of the NP with, for example, an antibody or aptamer to target a particular receptor on the surface of a cancer cell (Danhier et al., 2010). In addition to targeting and payload advantages, NPs can, in some cases, contribute to anticancer activity. They can also be loaded with nucleic acid therapeutics (NAT) and anticancer protein (ACP) in order to have multiple layers or modes of pharmacologic action. Much effort has been aimed at NP tumor targeting (Danhier et al., 2010; Li et al., 2015; Sykes et al., 2016; https://www.mccormick.northwestern.edu/news/articles/2017/05/first-spherical-nucleic-acid-drug-injected-into-humans-targets-brain-cancer.html; Tran et al., 2017; Liu et al., 2018; Rosenblum et al., 2018); however, a significant barrier in cancer nanomedicine remains with regard to effective metastases targeting. This review focuses on the anticancer mechanisms of the zinc oxide (ZnO) NP, a physiologically based metal-oxide NP our group has studied extensively, and what is currently known about its biologic activity. ZnO NPs have the ability to bind, stabilize, and deliver NAT and ACP, thus representing an exciting new strategy in combatting metastatic disease. It has become increasingly important to translate anticancer ZnO NAT or ZnO ACP beyond rodents and into spontaneously developing tumors in large animals such as pet dogs, which represent excellent comparative oncology models for multiple cancer types, including melanoma.

Advantages of ZnO NPs. A wide variety of NP types has been employed for drug delivery to melanoma as well as other cancer models in animals including, but not limited to, polymers, dendrimers, liposomes, polymeric micelles, nanogels, and microneedles targeting (Danhier et al., 2010; Cao et al., 2014; Li et al., 2015; Sykes et al., 2016; https://www.mccormick.northwestern.edu/news/articles/2017/05/first-spherical-nucleic-acid-drug-injected-into-humans-targets-brain-cancer.html; Tran et al., 2017; Liu et al., 2018; Rosenblum et al., 2018). Of the limited amount of data available to date, inorganic nanorod shapes are believed to have slightly higher tumor delivery efficiency than comparably sized and shaped organic, liposomal, or polymeric NP (Wilhelm et al., 2016). Our group has experience with gold (Au)-NP NAT delivery (DeLong et al., 2009, 2012) including its clinical translation (https://patents.justia.com/patent/8349364). However, thiol (-sulfhydryl) conjugation is in common use for Au NPs and is unnatural in nucleic acids. Disulfide bonds that stabilize protein structure may be disrupted upon Au-NP nanobio interaction. Instead, in cells and tissues, zinc is best known for stabilizing nucleic acid and protein interactions. In the nanoscale, metals such as zinc are known to oxidize to the metal oxide. Unlike other physiologic metals such as iron, cobalt, and manganese, a significant advantage of ZnO is that it exists in only one chemically stable form (ZnO). More importantly, in the last few years the unique indigenous anticancer activity of ZnO NPs has come to light (Rasmussen et al., 2010; Akhtar et al., 2012; Gopala Krishna et al., 2016; Moon et al., 2016; Mishra et al., 2017). Thus, in the next sections we review what is currently known about the mechanisms of ZnO NP anticancer activity and its biochemical activity and experience in animal models, with a future focus on nanomedicines designed to target NAT and ACP to melanoma and potentially other cancers.

Anticancer Properties of Zinc Oxide

Although the mechanisms by which ZnO exhibits selective anticancer properties are incompletely understood, several themes are beginning to emerge. These include cancer cell susceptibility due to the unique surface chemistry, reactive oxygen species (ROS) generation, intracellular gradients of free zinc ions, and biochemical effects on enzyme activity.

ZnO Surface Chemistry. ZnO is thought to be selective for cancer cells, in part due to its unique surface chemistry. ZnO NPs have been shown to be approximately 28–35 times more toxic to neoplastic T cells than normal cells, suggesting cancer-selective cytotoxicity as one of their innate characteristics (Hanley et al., 2008). These data are consistent with our work, where we reported a 39:1 selectivity ratio in melanoma (DeLong et al., 2017). Using reactive molecular dynamic simulations, we reported that ZnO can form $ZnOH_2^+$, leading to positive zeta potential surface charge analysis in water suspension (Thomas et al., 2018). At low pH, which occurs in cancer cells, this effect should be amplified. Because cancer cells have a higher concentration of anionic phospholipid, the positive charge of $ZnOH_2^+$ may drive electrostatic interactions at the membrane. Current dogma suggests that this property may underlie both the anticancer and drug delivery properties of ZnO NPs. The surface chemistry of ZnO NPs may also be related to their anticancer activity and ability to induce apoptosis in cancer cells (Akhtar et al., 2012).

Reactive Oxygen Species Generation. Zinc oxide is known to generate ROS, which induces apoptosis in cancer cells (DeLong et al., 2010; Akhtar et al., 2012). This is another cancer-selective property since rapidly dividing cells are more susceptible to biomolecular and organellar destruction caused by ROS. The presence of ROS induces redox cycling cascades and depletes the cellular reserve of antioxidants (Akhtar et al., 2012). Once these reserves have been depleted, the presence of ROS will induce apoptosis (Akhtar et al., 2012). In comparing the redox potential of various physiologic metal oxide NPs, linear regression analysis suggests that this parameter is correlated with ZnO NP antibacterial activity (Dai et al., 2018). In a comprehensive comparison of BEAS-2B transformed lung cells versus macrophages (RAW 264.7), physiologically based ZnO or cobalt oxide NPs compared favorably versus other metal oxide NPs in terms of the slope of their EC_{50}; however, both NPs exhibited a broad ROS heat map (Zhang et al., 2012). This aspect likely, again, implicates ZnO NP oxidative activity as an additional mechanism for its cancer cell–selective cytotoxicity.

Intracellular Gradients of Free Zn Ions. Toxicity of ZnO NPs to cancer cells has also been partially attributed to the accumulation of Zn^{2+} in the cytosol of cancer cells (Gopala Krishna et al., 2016; Moon et al., 2016). Intracellular, cytosolic concentrations of free zinc cations are low and strictly regulated by homeostatic variables (Rasmussen et al., 2010). Normal cells reuse and recycle, sequester, or excrete increased Zn concentrations; however, cancer cells, with unregulated growth and malfunctioning cellular metabolism, may be more susceptible to these ionicity-based mechanisms (Gopala Krishna et al., 2016; Moon et al., 2016).

Biochemical Effects on Enzyme Activity. Reports suggest that zinc and magnesium oxide NPs may act as catalysts (Lin et al., 2009; Ganguly et al., 2011). There are many classes of enzymes within cancer cells that catalyze important biochemical reactions for cell metabolism, growth, division, etc. Indeed, the effects of NPs on tumor biochemistry and cancer immunology are a critical gap in our knowledge. However, the impact of NPs on the enzymes that regulate these activities is likely an important aspect of their anticancer activity.

At present, there is extensive literature regarding protein interaction to NPs, and the mechanisms of protein and RNA nanobio interaction to a variety of physiologic metal oxides have been characterized (Gann et al., 2010; Barber et al., 2011; Canoa et al., 2015; DeLong et al., 2017; Simpson et al., 2017; Thomas et al., 2018). The ZnO NP interaction to protein enzymes inhibits biochemical activity, including model enzymes belonging to the hydrolase class (Cha et al., 2015; McCall et al., 2017) and the oxido-reductase class (Thomas et al., 2018). Enzymes from these two classes are important in cancer cell metabolism; when secreted, they can assist in cellular invasion by degrading components of the extracellular matrix. Enzymes in the RAS signaling pathway are activated in many aggressive cancers, and in melanoma this is hallmark. Importantly, we reported on the phosphorylation of extracellular signal–regulated kinase (ERK) and protein kinase B (AKT) enzymes (DeLong et al., 2017). These data strongly suggest that the ability of ZnO NPs to inhibit enzymes that drive cancer cell progression, drug resistance, and metastasis is of fundamental importance in their anticancer mechanisms. Figure 1 illustrates a cancer cell such as melanoma in the presence of ZnO NPs and the associated anticancer mechanisms (Fig. 1). As shown in Fig. 1, accumulating evidence suggests multiple mechanisms of anticancer activity for ZnO NPs including: 1) unique surface-forming $ZnOH_2^+$ interacting to anionic cancer cell membrane, 2) ROS-induced apoptosis, 3) tumor pH-dependent Zn^{++} disrupting ion homeostasis, and 4) enzyme inhibition.

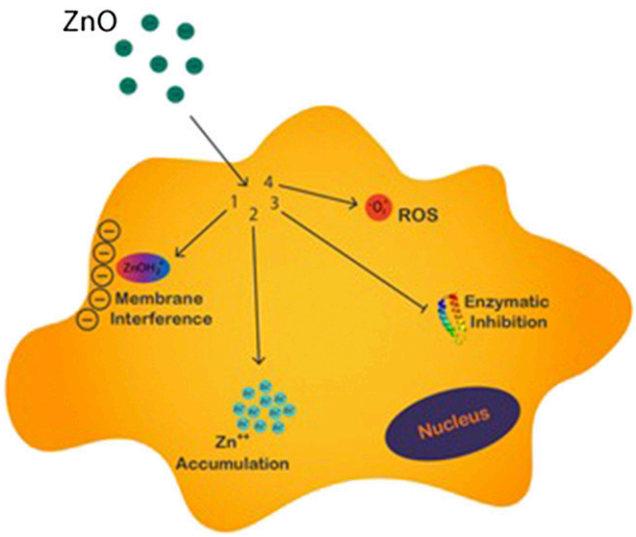

Fig. 1. Anticancer activity of ZnO NPs. Anticancer mechanisms include ROS, membrane interference, pH-dependent zinc ion flux or gradients, and enzyme inhibition.

Biologic Activity of ZnO NPs in Animal Models

Very little work has been done thus far on ZnO NPs in vivo, with much of the literature focused on Au, silicate, and iron oxide (Fe_3O_4) NPs (Benezra et al., 2011; DeLong et al., 2012; Hue et al., 2015; Lellouche et al., 2015; Poon et al., 2015; Du et al., 2018). Characterization of the conjugates was shown to be less than 100 nm by transmission electron microscopy and dynamic light scattering. Treated mice experienced no significant weight loss in comparison with control mice and drug could be detected in the plasma for up to 50 hours (Du et al., 2018). In another study, Au NPs were functionalized with polyethylene glycol (PEG) and/or peptide derived from myxoma virus (MDDRWPLEYTDDTYEIPW) or cyclic arginine-glycine-aspartic acid targeting integrin, which can be confirmed by shifts in the zeta potential surface charge and the molar ratio of peptide to Au NPs based on absorbance spectroscopy. In this case, Au-NP conjugation to the peptide did not appear to impact cell survival, which is consistent with our results for Au-NP short interfering RNA delivery (DeLong et al., 2012; Poon et al., 2015). However, functionalization did have a dramatic effect on tissue distribution, specifically early tumor accumulation, clearance from the blood, and urine excretion in the B16 melanoma grafted on C57/BL6 mice (Poon et al., 2015). In another study, Nu/Nu mice bearing human M21 melanoma were administered silica NPs radiolabeled with iodine-124; based on radiation dosimetry data, 6.4% of the injected dose was detected within the untargeted and 8.9% within the targeted tumor tissue (Benezra et al., 2011), which is somewhat higher than recent meta-analysis would suggest (Wilhelm et al., 2016). Bioimager analysis of Cy5.5-labeleled thermally crosslinked iron oxide suggested organ distribution was in the following order: liver > spleen~lung > kidney > blood > stomach > brain > lymph node > all other organs, based on fluorescent signals in these tissues several hours after intravenous administration (Hue et al., 2015). It should be noted that after 3 days, fluorescence in the liver and spleen accounted for >90% of the residual fluorescence with near background levels in all other tissues except kidney and lung. These data may have profound implications for NP targeting, especially for cancers originating in these organs or those with propensity to metastasize to the liver or lung, such as melanoma. Recently, maghemite NPs doped with lanthanide, referred to as magnetic reagent for efficient transfection NPs, have been assessed. When functionalized with polyethyleneimine, magnetic reagent for efficient transfection NPs penetrate SK-OV-3 cells as shown by confocal fluorescence microscopy. Therefore, when loaded with short interfering RNA, these NPs could silence both marker and cancer-associated genes (Lellouche et al., 2015). Importantly, polyethyleneimine toxicity could be greatly mitigated by ligation to short interfering RNA functionalized magnetic reagent for efficient transfection. These data strongly support NP surface activity, as performed here with RNA functionalization, in the underlying anticancer mechanism.

The Case for Zinc Oxide Nanoparticles. Inorganic NPs are thought to have slightly higher tumor delivery efficiency than comparable sized or shaped liposome or polymer nanomaterials (Wilhelm et al., 2016). Data are beginning to emerge that indicate the anticancer activity of ZnO NPs observed in in vitro models may extend into in vivo rodent models. One group synthesized core-shell NPs (CSNPs) of Fe_3O_4-ZnO and tested this CSNP in tumor-bearing DBA/2 mice. After peritumoral injection of the CSNP, tumor growth inhibition

TABLE 1
Effects of ZnO-based NPs in rodents

NP	Synthesis	Characterization	Animal Model	Biologic Activity	Reference
Fe-doped ZnO	Atomization of zinc or iron napthenate with CH_4/O_2 combustion	TEM	DBA/2 Mice bearing KLN 205 tumor	Luciferase expressing KLN 205 cells showed tumor growth was inhibited more after peritumoral injection with higher percentages of ZnO relative to Fe.	Wilhelm et al. (2016)
Fe_3O_4-ZnO CSNP	Modified nanoemulsion method	TEM (<100 nm) DLS (>100 nm), ZP −16 to −25 mV (in PBS)	C57BL/6 mice	Hematology, serum biochemistry, and organ Zn was assayed by ICP-AES after subcutaneous injection of 4 and 20–200 mg/kg. Some agglomeration and granulomas were observed but no other dose-dependent overt toxicity was reported.	Manshian et al. (2017)
Cy5.5-ZnO	Cy5-NHS reacted with citrate-ZnO-EDEA	FTIR and optical images of Cy5.5-ZnO NP	Sprague-Dawley Rats	Micro-, nano-ZnO, or dye control was compared after oral administration. Cy5.5 blood concentration peaked at 5 h, and at 7 h was in the order: kidney > liver > lung ~ pancreas > all other tissues	Yun et al. (2015)
ZnO	Purchased from Sigma-Aldrich	None shown	Female ICR mice (CLEA, Japan)	A single 0.05 or 0.2 mg/kg dose was given via the tail vein. Zn levels in the blood were followed at 20, 40, and 60 min, and were in the order: spleen ≥ lung ≥ kidney ≥ liver at days 1, 3, and 6.	(Lee et al., 2012)
ZnO	Purchased from Sigma-Aldrich	None shown	In-bred strains of female Balb/c	A single 500 μl intraperitoneal injection of 0.25, 0.5, 1, or 3 mg ZnO NP. Anaphylaxis score was ZnO < Ova < ZnO-Ova (20% of the ZnO NP mice rubbed their eyes and snout). Histologic differences in the lung, intestine, and spleen were observed and changes in IL-2, 4, 6, 10, and 17; TNF-a; and MHC I and II were observed, presumably at the highest dose.	Fujihara et al. (2015)
ZnO	Wet chemical Zn-nitrate/NaOH,	ZP near neutral; EM and DLS ≥100 nm	BALB/c	After oral gavage with 200 mg/kg, 100% survived, with no change in neutrophil, eosinophil, or lymphocyte at day 1 or 6.	Roy et al. (2014a,b)
NOTA-ZnO-PEG-TRC105 (targeting antibody)	Calcination followed by thiol conversion and maleimide reaction to attach PEG and targeting agent, filter purified, washed with water and ethanol	TEM, fluorescence spectrum	BALB/c bearing murine breast 4T1 tumor	TRC105 functionalized conjugates increase cell association as shown by CFM. Using PET analysis of Cu-64 conjugates, tumor uptake varies from 6% of administered dose initially to about 4% after 24 h. Histologic analysis confirmed tumor uptake.	Hong et al. (2015)
ZnO-Gd-Dox	Zinc methacrylate reacted with AIBN and PEG-methyl ether methacrylate	TEM, UV and T1-weighted MR, and UV and PL spectra	BxPC-3 tumor-bearing nude mice	Tumor volume growth vs. initial volume was significantly reduced for ZnO-Gd-Dox vs. controls, Significant histologic improvement in tumor.	Ye et al. (2016)

AIBN, azobisisobutyronitrile; CFM, confocal fluorescence microscopy; DLS, dynamic light scattering; Dox, doxorubicin; EDEA, *N*-ethyldiethanolamine; FTIR, Fourier-transform infrared spectroscopy; Gd, gadolinium; ICP-AES, inductively coupled plasma atomic emission spectroscopy; ICR, Institute of Cancer Research; IL, interleukin; MHC, major histocompatibility complex; MR, magnetic resonance; NOTA, $C_{12}H_{21}N_3O_6$; PET, positron emission tomography; PL, photoluminescence; TEM, transmission electron microscopy; TNF, tumor necrosis factor; ZP, zeta potential.

increased with increasing zinc percentage of the CSNP (Wilhelm et al., 2016). Another group tested the toxicity of Fe_3O_4-ZnO CSNPs in C57BL/6 mice receiving subcutaneous injections of 4, 20, or 200 mg/kg dosages of Fe_3O_4-ZnO CSNPs. These mice exhibited no toxicity, with no significant weight loss or food and water consumption changes noted (Manshian et al., 2017). Table 1 presents an overview of ZnO NP data in mice to date. The nanomaterial synthesis and characterization, as well as the animal model in which testing was performed and the biologic activity data in each model, are briefly summarized.

As shown in Table 1, dosages from 0.05 to 200 mg/kg were tested in mice or rats. Thus far, the synthesis or conjugation method has not been standardized, although both PEG and Cy5.5 tracking dye have been tested, as previously mentioned, with excellent results. The data, thus far, suggest that bioavailability in kidney, liver, lung, and spleen is good. Although little information is available on tumor uptake, two reports suggest significant tumor uptake and histologic improvements of the tumor (Hong et al., 2015; Ye et al., 2016). However, as can be seen there is some interest in doping or functionalizing ZnO NPs, and a variety of different synthetic procedures and characterization methods have been employed. At present, none of these have been standardized nor have they been compared in a standard animal or tumor-bearing model, thus there remains a great deal of work to be done for in vivo assessment of ZnO NPs.

Effect of ZnO or ZnO-RNA on Experimental Melanoma in Mice. Currently, there is interest in the nexus between cancer immunology and nanotechnology. The anticancer and immunogenic properties of polyinosinic:polycytidylic acid (poly I:C), a synthetic analog of double-stranded RNA, has long been known. Our group first reported combined antitumor activity of ZnO NPs with poly I:C in the immunocompetent B16F10-BALB/c experimental melanoma mouse model (Ramani et al., 2017a). Analysis of the tumor proteome within this model at the time of metastasis revealed significant ERK and AKT activation in the mice, consistent with what is reported for malignant melanoma in the National Cancer Institute Cancer Genome Atlas (https://cancergenome.nih.gov/cancersselected/melanoma). We observed that the ZnO or ZnO/poly I:C NP significantly suppresses the phosphorylation of both these key downstream drivers of melanoma in the mouse model (Fig. 2).

As shown in Fig. 2, the majority of human melanomas analyzed by the National Cancer Institute Cancer Genome Atlas have an altered NF1-RAS-BRAF axis, where drug resistance has been linked to an altered splicing and protein interaction in the Ras-binding domain (RBD). Ultimately, this leads to activation of ERK and AKT and is associated with melanoma progression and metastasis. Injection of either ZnO NP or ZnO-poly I:C complexes directly into the tumor causes tumor regression. Analysis of these key drivers of melanoma revealed substantial abatement of both enzymes' phosphorylation, albeit ERK is only partially blocked. These results suggest that either NAT or ACP, targeting RAS or RBD, could suppress ERK activation altogether and lead to complete melanoma regression.

Pharmacokinetics of ZnO NPs

Pharmacokinetics and Biodistribution of ZnO NPs in Healthy Animals. Pharmacokinetics (PKs) is the science of studying the rate and extent of absorption, distribution, metabolism, and elimination of chemicals, drugs, or NPs by systemically and quantitatively using experimental and mathematical approaches (Riviere, 2009; Choi and Choy, 2014; Lin et al., 2015). PK data provide critical information about the entry of NPs into systemic circulation (bioavailability), their distribution (volume of distribution), and accumulation in the target organs (C_{max} and area under the time-concentration curve), as well as the time required for clearance (mean residence time, clearance, and half-life). A comprehensive review of the PK information of delivered NPs will contribute to designing an optimal therapeutic with higher delivery efficiency to target organs and tissues, maintaining desired therapeutic time, and avoiding unwanted toxicity.

Baek et al. (2012) and Paek et al. (2013) investigated the pharmacokinetics and biodistribution of various sizes of ZnO NPs (20 and 70 nm) in Sprague-Dawley rats following a single oral administration. Their results showed that the absorption profiles in rat plasma were dose dependent with approximate absorption efficiency estimates to be 13%, 25%, and 31% after oral exposure to 50, 300, and 2000 mg/kg of negatively charged ZnO NPs, respectively (Baek et al., 2012). However, no significant differences in absorption efficiency were demonstrated between NP size and gender. Similar dose dependency was identified in rat plasma after rats orally received the same doses of positively charged ZnO NPs with lower absorption efficiency estimates of 11%, 15%, and 16%, respectively (Paek et al., 2013).

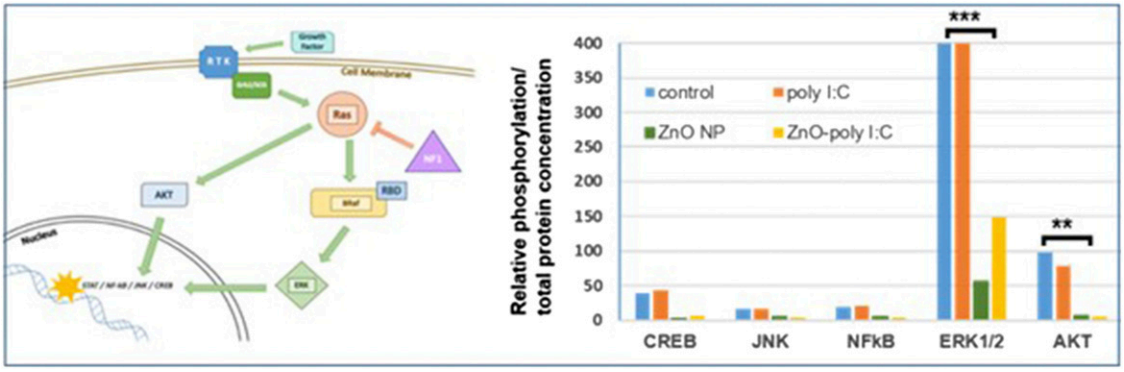

Fig. 2. Altered NF1-RAS-BRAF axis and interactions in RBD lead to downstream ERK and AKT activation in melanoma tumor at-the-time-of-metastasis [adapted from Ramani et al. (2017a,b) and DeLong et al. (2017)].

Tissue distribution profiles suggest that orally administered ZnO NPs tend to accumulate in lungs, liver, and kidneys of rats, regardless of NP size, surface charge, or gender (Baek et al., 2012; Paek et al., 2013). Long-term exposure of 50, 500, and 5000 mg/kg ZnO NPs added in the diet of Institute of Cancer Research mice from week 3 to 35 suggests higher Zn accumulation in liver, pancreas, kidney, and bones (Wang et al., 2016). After intravenous injection of 10 and 71 nm neutron-activated ^{65}ZnO NPs, the liver, spleen, kidneys, and lungs were determined to be target organs with 10 nm ^{65}ZnO NPs being most widespread in lungs, revealing a size-varied biodistribution effect (Yeh et al., 2012). Li et al. (2012) reported that 93 nm ZnO NPs in male Institute of Cancer Research mice following intraperitoneal injection were more effectively distributed to liver, spleen, kidneys, lungs, and heart, compared with their distribution to liver, spleen, and kidneys after oral administration. In summary, liver and kidneys are likely to be common target organs, regardless of the various physicochemical properties of ZnO NPs, administration routes, and experimental species. Note that the primary excretion pathway of Zn is via feces, while urinary excretion through kidneys only plays a minor role following different administration routes (Baek et al., 2012; Yeh et al., 2012; Paek et al., 2013; Choi et al., 2015).

Pharmacokinetics and Biodistribution of ZnO NPs in Tumor-Bearing Animals. Over the past decade, unique physicochemical and biologic properties of engineered NPs have led to key biomedical applications for diagnosis and cancer targeting therapy. However, the translation of nanomedicine into clinical applications is limited partly due to low delivery efficiency to the tumor and lack of knowledge on the quantitative effects of various physicochemical factors of NPs on tissue/tumor distribution. Therefore, systemic understanding of PKs in NP delivery to tumor using mathematical approaches may significantly contribute to NP-based anticancer drug design with higher tumor delivery efficiency and optimal therapeutic index (Wilhelm et al., 2016). In view of the optimal design of nanomedicine with higher targeting power in cancer therapy with lower toxicity, the biodistribution of administered Zn-associated NPs with increased accumulation in the tumor and decreased accumulation in normal tissues, especially for liver and kidneys, is desired (Nicolas et al., 2013). There are only limited PK studies using Zn-based NPs to investigate the NP tissue/tumor biodistribution in tumor-bearing animals. The focus of this review is on representative articles associated with the effects of various NP physicochemical properties and targeting strategies (i.e., passive vs. active targeting) on tumor delivery efficiency of ZnO NPs.

Hong et al. (2015) employed radiolabeled targeting ligand (TRC105) conjugated ZnO NPs to examine the differences in tumor delivery efficiency between passive (^{64}Cu-$C_{12}H_{21}N_3O_6$-ZnO-PEG-NH_2) and active targeting NPs (^{64}Cu-$C_{12}H_{21}N_3O_6$-ZnO-PEG-TRC105) at 0.5, 3, 16, and 24 hours following intravenous injection using a positron emission tomography imaging method. Comparing the differences in tumor accumulation, there was an approximate 2.5-fold enhancement in tumor delivery efficiency with active targeting TRC105 nanoconjugate of 4.9% of the injected dose per gram of tissue over passive targeting ZnO NPs of 1.9% of the injected dose per gram of tissue at 24 hours post intravenous injection into 4T1 tumor-bearing mice. In addition, the uptake of ^{64}Cu-$C_{12}H_{21}N_3O_6$-ZnO-PEG-TRC105 was demonstrated mainly in the 4T1 tumor compared with the major organs or tissues except liver and spleen that were responsible for primary clearance. Higher tumor accumulation of active targeting doxorubicin-loaded folate conjugated Zn(II)-crosslinked polymeric nanohydrogels (FPZCLNs-15) was also indicated by Zhang et al. (2016) compared with the accumulation of passive targeting NPs (PZCLN-15) in the H22 tumor in tumor-bearing mice following intravenous injection (~1.4-fold higher). It is worth noting that a favorable biodistribution with lower doxorubicin accumulation in liver and kidneys and higher tumor delivery was demonstrated in Zhang et al. (2016).

Physiologically Based Pharmacokinetic Model for ZnO NPs. Besides traditional pharmacokinetic analyses, another technique that can integrate and compare PK data derived from healthy and tumor-bearing animal studies in order to gain deeper insights into the biodistribution and tumor delivery of administered NPs is physiologically based pharmacokinetics (PBPK) modeling (Li et al., 2010, 2017; Lin et al., 2015). PBPK modeling is a mechanistic and mathematical modeling approach based on the physicochemical properties of NPs coupled with anatomy and physiology within a living body with organs and tissues interconnected by blood flow to characterize the process of absorption, distribution, metabolism, and elimination. The advantages of implementing PBPK models include their great extrapolation power across doses, routes, and species, as well as the ability to predict target tissue and in-site tumor dosimetry from various external administrations, which is important in nanomedicine applications. Among the few available PBPK models developed for metallic NPs (Lankveld et al., 2010; Bachler et al., 2015; Chen et al., 2015; Carlander et al., 2016; Lin et al., 2016a,b), only one PBPK modeling study was developed to describe the tissue biodistribution of ZnO NPs in healthy mice (Chen et al., 2015). Chen et al. (2015) developed a perfusion-limited PBPK model for healthy mice to simulate the target tissue pharmacokinetics of 10 and 71 nm ^{65}ZnO NPs and $^{65}Zn(NO_3)_2$, including blood, brain, lungs, heart, spleen, liver, gastrointestinal tract, kidneys, and carcass up to 28 days after intravenous injection via tail vein. Specifically, they estimated the time-dependent partition coefficients and excretion rates based on previously published biodistribution data of healthy mice. The developed PBPK model reasonably predicted target tissue distribution of ZnO NPs with mean absolute percentage of error estimates of $<50\%$. Currently, there is no PBPK modeling framework available for tumor-bearing animals to simulate nontumor and tumor tissue distribution and to facilitate the design of new NP-based anticancer drugs with higher tumor targeting efficiency and optimal therapeutic index. To gain more insight into the PKs of delivered ZnO NPs in nontumor as well as in-site tumor tissues in tumor-bearing animals, a PBPK modeling framework in tumor-bearing animals needs to be developed, which is our future direction.

Comparative Oncology

Animal models have long provided the means to test novel anticancer agents and diagnostic modalities in a preclinical setting. Such animal models function as the final filters in selecting drugs for clinical trials. Although rodents are most frequently used in this setting, and do provide some distinct advantages in terms of experimental tractability, there are also well-recognized limitations of the mouse model. Murine

models often lack key characteristics of human cancers, such as long latency, genomic instability, and heterogeneity among the tumor cells and the surrounding microenvironment. Consequently, the immensely complex biology of cancer development, recurrence, and metastasis is not sufficiently recapitulated in mice, and unfortunately these limitations are often reflected in the unacceptably high drug candidate attrition rate of subsequent clinical trials (Hansen and Khanna, 2004; Porrello et al., 2006; Paoloni and Khanna, 2007, 2008; Khanna et al., 2009; Gordon and Khanna, 2010; Rowell et al., 2011; Pinho et al., 2012; Alvarez, 2014; Nass and Gorby, 2015; Schiffman and Breen, 2015; LeBlanc et al., 2016).

Larger animal models, specifically dogs, have been gaining traction over the preceding decade as preclinical and early clinical models to facilitate the drug and diagnostic development pathway, and our canine companions possess several advantages over traditional rodent models (Hansen and Khanna, 2004; Porrello et al., 2006; Paoloni and Khanna, 2007, 2008; Khanna et al., 2009; Gordon and Khanna, 2010; Rowell et al., 2011; Pinho et al., 2012; Alvarez, 2014; Nass and Gorby, 2015; Schiffman and Breen, 2015; LeBlanc et al., 2016). Of the approximately 70 million pet dogs in the United States, it is estimated that one in four will develop cancer during their lifetime, and nearly 50% over the age of 10 years will die as a result (Bronson, 1982; Adams et al., 2010). Dogs spontaneously develop many of the same malignancies as people as they age, and have intact immune systems compared with rodent models. Because they are physiologically similar, share environmental exposures without unhealthy habits, and have access to high level healthcare, dogs function as ideal comparative models for human disease. Canine and human tumors also share genetic complexity, overlapping mutations, similar tumor microenvironments, potential for therapeutic resistance, and in many cases similar responsiveness to conventional therapeutics. When practically considered, cancer evolves comparatively quickly in the dog, such that the time from carcinogen exposure to disease development is shorter, disease progression is more rapid, and therapeutic responses are observed more expeditiously; therefore, answers to critical questions can be obtained more readily and cost effectively (Hansen and Khanna, 2004; Porrello et al., 2006; Paoloni and Khanna, 2007, 2008; Khanna et al., 2009; Gordon and Khanna, 2010; Rowell et al., 2011; Pinho et al., 2012; Alvarez, 2014; Nass and Gorby, 2015; Schiffman and Breen, 2015; LeBlanc et al., 2016).

Several canine cancers have demonstrated applicability as translational models (Gordon et al., 2009) including non-Hodgkin's lymphoma (Ito et al., 2014), osteosarcoma (Simpson et al., 2017), urothelial cell carcinoma (Knapp et al., 2014), brain tumors (Hicks et al., 2017), and malignant melanoma (Hernandez et al., 2018). These canine tumors share histologic appearance, genetic and/or molecular aberrations, biologic behavior, and response to specific therapeutics with their human counterparts (Gordon et al., 2009; Ito et al., 2014; Knapp et al., 2014; Hicks et al., 2017; Simpson et al., 2017; Hernandez et al., 2018). A pertinent example is malignant melanoma (Hernandez et al., 2018). In humans, melanoma most often arises in the skin and is associated with lack of pigmentation and UV light exposure. It is estimated that it will be responsible for approximately 10,000 cancer-related deaths this year alone in the United States (American Cancer Society, 2018). Melanoma is diagnosed in nearly 100,000 dogs per year in the United States (Bergman et al., 2013) and most commonly develops in the oral mucosa. Oral melanomas typically exhibit aggressive local behavior and frequent metastasis (Sulaimon and Kitchell 2003; Kunz, 2014), warranting a poor prognosis with short survival times for affected animals. Currently, the management of melanoma in dogs is similar to the disease in humans with initial therapy aimed at local disease control, utilizing a combination of surgery, radiation therapy, chemotherapy, and immunotherapy (Sulaimon and Kitchell 2003; Bergman et al., 2013; Kunz, 2014).

Human cutaneous melanomas often contain an activating BRAF mutation (Davies et al., 2002; Ascierto et al., 2012; Kunz, 2014), resulting in constitutive mitogen-activated protein kinase pathway activation. Other activating mutations recognized include RAS (~20%) (Kelleher and McArthur, 2012), NF1 (~25%) (Kiuru and Busam, 2017), and occasionally KIT (Curtin et al., 2006). However, some have no documented mutations and are considered triple wild-type melanoma (Cancer Genome Atlas Network, 2015). The similarities between human and canine melanoma were compared by the Comparative Melanoma Tumor Board (Simpson et al., 2014), which found substantial common characteristics between human mucosal and canine melanoma (Simpson et al., 2014; Fowles et al., 2015) and confirmed that canine melanoma dysregulates and constitutively activates the mitogen-activated protein kinase and PI3K/AKT pathways.

With evidence of activation of the same molecular pathways in human and canine melanoma, canine malignant melanoma is an excellent translational model for drug-resistant BRAF-mutated melanoma as well as melanoma with a triple wild-type phenotype (Simpson et al., 2014; Fowles, et al., 2015; Hendricks et al., 2018). Because of the disease similarities, the dog provides an outstanding model for further investigation into melanoma pathogenesis as well as the development of urgently needed novel therapeutic interventions for this devastating disease in dogs and humans alike.

Conclusions and Outlook. In conclusion, nanomedicines are becoming a vital new weapon in the cancer treatment arsenal. This is especially important for highly metastatic cancers such as melanoma, where treatment options beyond the newer kinase inhibitors and immunotherapies are currently limited. One approach gaining acceptance within the community that presents a potential solution to this complex problem is to use a physiologically based nanoparticle with intrinsic or indigenous anticancer properties, such as ZnO, and to load it for delivery with NAT and ACP, which can target the molecular basis for metastasis.

Such combinatorial bionanotechnology is an exciting possibility with a number of compelling and distinct advantages. As such, the surface properties of ZnO NPs provide a substrate to attach the NAT and ACP, yet also enable ROS, Zn ions, and membrane interactions, which underlie its anticancer activity. So, too, ZnO NPs can act as a direct enzyme inhibitor, in some cases inhibiting oxido-reductases, hydrolases, and synthetases generally thought to be important in cancer, or as is the case for treating melanoma with ZnO NPs, inhibiting transferases such as ERK and AKT kinases, which have been directly linked to melanoma progression and metastasis (DeLong et al., 2017; Ramani et al., 2017a; https://cancergenome.nih.gov/cancersselected/melanoma).

Although there is a limited data set for ZnO NPs in vivo, the data thus far appear very promising. Oral doses of

50–2000 mg/kg have been tested with bioavailability ranging from 11% to 31% and distribution in the liver, pancreas, kidney, and bones observed. After intraperitoneal administration of ZnO NPs, uptake was seen primarily in the liver and kidney but was also notable in lung and spleen. These data are highly favorable for delivery of NAT, ACP, or other types of anticancer therapies to cancer in these organs by ZnO NPs. Although there are very few studies thus far for ZnO NPs in mice, particularly tumor-bearing animals, based on the data shown in Table 1 these results look promising with tumor delivery efficiencies of more than the 0.9%–1% efficiency expected for inorganic NPs (Wilhelm et al., 2016). Furthermore, data for ZnO NPs loaded with doxorubicin suggest redirection of the drug from liver and kidney to the tumor, and targeting of ZnO NPs to tumor is facilitated by monoclonal antibody conjugation (Ye et al., 2016).

Comparative oncology studies in the dog as a model for melanoma and other cancers has a number of distinct advantages. These include (but are not limited to) latency of disease, genomic instability and heterogeneity, microenvironment surrounding the tumor, common cellular and molecular features, and others. Besides malignant melanoma, other cancers considered as comparative oncology models are non-Hodgkin's lymphoma (Hernandez et al., 2018), osteosarcoma (American Cancer Society, 2018), urothelial cell carcinoma (Chang et al., 1998), brain tumors (Bergman et al., 2013), and others. For malignant melanoma, clinical management is also similar in dogs and humans; however, the options for advanced disease are limited, making the search for a nanomedicine approach an important prerogative. Although the characteristic BRAF and RAS mutations are not prevalent in canine melanoma, constitutive activation of the mitogen-activated protein kinase and PI3K/AKT pathways is hallmark. Given that ZnO NP treatment significantly inhibits ERK and AKT activation of murine and human melanoma in cell culture and mice (Fig. 2), the activity of ZnO NPs on canine melanoma is of considerable importance and is currently being assessed.

On the Horizon. The ability of ZnO NPs to deliver biomacromolecules into cancer cells makes this treatment option an attractive mechanism by which to potentiate cancer therapy by combining its attractive anticancer activity with other drugs, NAT and ACP, or immunologically active compounds. Indeed, the excellent antitumor activity of zinc-doped superparamagnetic iron oxide nanoparticles combined with the anticancer immunopotentiator RNA, poly I:C, and small molecule, imiquimod, has recently been reported against experimental melanoma (Bocanegra Gondan et al., 2018). Zinc-doped superparamagnetic iron oxide nanocrystals exhibited excellent magnetic properties and could be visualized by magnetic resonance imaging after peritumoral administration. This combination protected against melanoma challenge and also had significant therapeutic activity against established disease. Hence, it is likely that such combination nanomedicines will be necessary to combat metastatic disease.

Due to their exquisite sequence selectivity, NAT delivery by ZnO NPs holds promise in targeting RAS and other important pathways contributing to cancer drug resistance and metastasis. Thus far, three classes of NAT have received clinical approval: antisense, splice switching oligomer, and aptamer, albeit, not yet for cancer indication (Gragoudas et al., 2004; Adams et al., 2017; Stein and Castanotto, 2017). Previously, we reported on antisense oligomer targeting K-RAS against experimental pancreatic cancer in mice (DeLong et al., 1997); however, for melanoma, as shown in Fig. 2, alterations in the NF1-RAS-BRAF nexus are implicated in the majority of human melanomas analyzed thus far by the National Cancer Institute Cancer Genome Atlas Program (https://cancergenome.nih.gov/cancersselected/melanoma). Furthermore, kinase inhibitor resistance in melanoma develops primarily due to splicing alterations in the RBD (Salton et al., 2015), which leads to altered interactions with RAS (Poulikakos et al., 2011). Since this is upstream of both ERK and AKT, this is a highly attractive target. To address this, we are studying the interaction and delivery of the RBD itself as a decoy, and have designed RBD-specific switching oligomer or aptamer sequences for targeting RAS by NAT (submitted manuscript Elza Neelima Mathew, Miranda N Hurst; Jayden H McCall; Baolin Wang; Vaibhav Murthy; Kartik C Ghosh; Robert K DeLong). As a first approach, we modified the full-length RBD aptamer with a phosphorothioate backbone, which has improved tumor delivery efficiency, target affinity, and in vivo stability (Cheng et al., 1997; DeLong et al., 1997). In this case, since its RBD interaction site is known and the bases implicated in RBD interaction have been identified by nuclease mapping (Kimoto et al., 2002), it was possible to retain these as RNA. The remaining structural portion of the molecule could be further stabilized by DNA substitution to create a DNA-RNA hybrid molecule replacing uracil with deoxyuridine (Fig. 3).

The RNAfold (Institute for Theoretical Chemistry, University of Vienna) computational prediction for the full-length RBD-specific aptamer, where target interaction is confirmed by gel shift, is shown in Fig. 3. Thus far, we do know that interaction of RNA (poly I:C) to ZnO NPs improves its resistance to RNase A digestion and degradation from exposure to serum, liver, or tumor homogenate (McCall et al., 2017). However, based on the ZnO NP strength of interaction to the RBD ($K_d < 10^{-5}$) and the fact that this interaction inhibits enzyme activity (Cha et al., 2015; McCall et al., 2017; Thomas et al.,

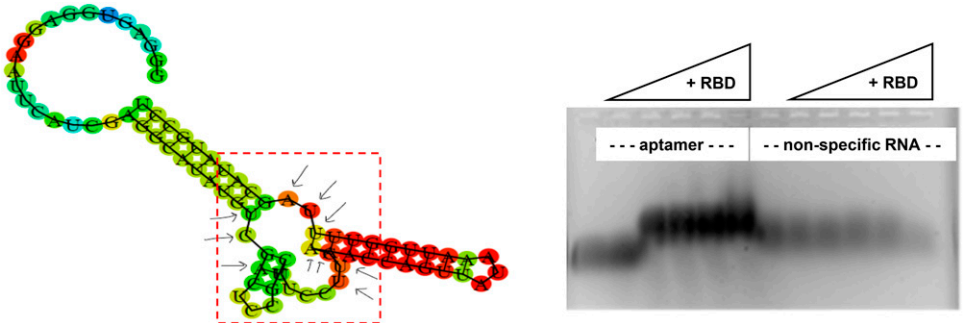

Fig. 3. (Left) RNAfold predicted structure for full-length RBD-specific aptamer with interaction site in the hashed box and bases known to interact with RBD retained as RNA indicated by arrows. (Right) Specificity of its interaction to RBD is shown by the gel shift with micromolar affinity vs. nonspecific RNA control (torula yeast RNA). RBD was tested at 0, 1:10,000, 1:1000, 1:100, or 1:10 dilution of stock at constant RNA concentration (100 μg/ml).

2018), its impact on RNA structure, function, and activity is at present a critical unknown. When ZnO NPs are incubated with either torula yeast RNA or poly I:C, we observe a distinct gel shift with an associated change in fluorescence intensity, suggesting a strong interaction between the NP and RNA (Ramani et al., 2017a,b; unpublished data). However, the mechanism of ZnO NP RNA interaction and structure-function impact is poorly understood. Based on our Raman and Fourier-transform infrared spectroscopy studies of ZnO NP interaction to adenosine triphosphate or inosine and cytosine model molecules, stabilizing ionic interactions occur primarily through the phosphodiester backbone but also through what appear to be hydrogen bond–type interactions to the various nucleic acid functional groups (Bhaumik et al., 2014; Ramani et al., 2017b). However, based on our recent liquid chromatography analysis, amino acid interactions to ZnO NPs appear to be much more complex (Thomas et al., 2018) and need to be further studied for both NAT and ACP. When poly I:C is incubated in the presence of ZnO NPs and analyzed by circular dichroism spectroscopy, there appears to be little structural disturbance (submitted manuscript; R. K. DeLong, Elza Mathew et al,). Recently, we patented two-dimensional fluorescence difference spectroscopy as a new quality control assay for measuring nanoparticles, and more importantly their biomolecular interaction (Hurst and DeLong, 2016; DeLong and Hurst, 2018). Based on two-dimensional fluorescence difference spectroscopy, utilizing a magnesium-doped ZnO NP synthesized by our collaborator, we do see evidence that the surface of the ZnO NP enables coattachment of both aptamer and its protein target (Hurst and DeLong, 2016). Furthermore, in the case of the most well-characterized aptamer-thrombin system, introduction of ZnO NPs does not appear to interfere with the binding isotherm of this interaction (Hurst and DeLong, 2016). However, it remains to be seen whether NAT- or ACP-bound ZnO NPs are physicochemically stable in biologic media, are able to functionally deliver these biomacromolecules in order to retain target interaction and biochemical activity in cells and tissues, and ultimately be used for effective tumor or metastasis delivery in vivo. This is, quite obviously, an important research goal moving forward.

Targeting Metastases. Despite a strong body of literature utilizing antibody-targeted NPs for drug delivery to tumor (Li et al., 2015; Liu et al., 2018), there is a movement to simplify the use of antibodies by using synthetic, less immunogenic substitutes; for example, using RNA such as poly I:C, aptamer, or shorter peptides. These may contribute less untoward autoimmunity, which will limit the ability to readminister the nanomedicine. Use of poly I:C–targeted superparamagnetic iron oxide nanocrystals may improve delivery to the lymphatic system (Cobaleda-Siles et al., 2014), which is a common site of metastasis. Although poly I:C TLR3 signaling is well known, other receptors such as MDA5 and signaling mediated by antibacterial peptide LL-37, may target the surface of both lung and metastatic melanoma cells (Singh et al., 2013; DeLong and Curtis, 2017; Jia et al., 2017). Anticancer activity is associated with a portion of the LL-37 sequence, which bears significant homology with several other ACP classes (Felicio et al., 2017). These data suggest that LL-37–derived ACP may serve as a melanoma-specific or lung cancer–selective targeting peptide. Through comparative proteomics analysis, it may be possible to design metastasis-targeting peptides in order to better address multifunctionalized anticancer NPs for delivery to sites of metastases in the creation of antimetastatic nanomedicines.

Acknowledgments

R.K.D. acknowledges the start-up received from the Nanotechnology Innovation Center at Kansas State, which supported E.N.M. and A.H.

Authorship Contributions

Participated in research design: Pearson, Hoffman, Mathew, DeLong.
Conducted experiments: Cheng, Lin, Coffee, Wouda, Higginbotham.
Wrote or contributed to the writing of the manuscript: Higginbotham, DeLong.

References

Adams VJ, Evans KM, Sampson J, and Wood JLN (2010) Methods and mortality results of a health survey of purebred dogs in the UK. *J Small Anim Pract* **51**: 512–524.
Adams BD, Parsons C, Walker L, Zhang WC, and Slack FJ (2017) Targeting non-coding RNAs in disease. *J Clin Invest* **127**:761–771.
Akhtar MJ, Ahamed M, Kumar S, Khan MM, Ahmad J, and Alrokayan SA (2012) Zinc oxide nanoparticles selectively induce apoptosis in human cancer cells through reactive oxygen species. *Int J Nanomedicine* **7**:845–857.
Alvarez CE (2014) Naturally occurring cancers in dogs: insights for translational genetics and medicine. *ILAR J* **55**:16–45.
American Cancer Society (2018) *Cancer Facts & Figures 2018*, American Cancer Society, Atlanta, GA.
Ascierto PA, Kirkwood JM, Grob JJ, Simeone E, Grimaldi AM, Maio M, Palmieri G, Testori A, Marincola FM, and Mozzillo N (2012) The role of BRAF V600 mutation in melanoma. *J Transl Med* **10**:85–93.
Bachler G, von Goetz N, and Hungerbuhler K (2015) Using physiologically based pharmacokinetic (PBPK) modeling for dietary risk assessment of titanium dioxide (TiO_2) nanoparticles. *Nanotoxicology* **9**:373–380.
Baek M, Chung HE, Yu J, Lee JA, Kim TH, Oh JM, Lee WJ, Paek SM, Lee JK, Jeong J, et al. (2012) Pharmacokinetics, tissue distribution, and excretion of zinc oxide nanoparticles. *Int J Nanomedicine* **7**:3081–3097.
Barber S, Abdelhakiem M, Ghosh K, Mitchell L, Spidle R, Jacobs B, Washington L, Li J, Wanekaya A, Glaspell G, et al. (2011) Effects of nanomaterials on luciferase with significant protection and increased enzyme activity observed for zinc oxide nanomaterials. *J Nanosci Nanotechnol* **11**:10309–10319.
Benezra M, Penate-Medina O, Zanzonico PB, Schaer D, Ow H, Burns A, DeStanchina E, Longo V, Herz E, Iyer S, et al. (2011) Multimodal silica nanoparticles are effective cancer-targeted probes in a model of human melanoma. *J Clin Invest* **121**: 2768–2780.
Bergman PJ, Kent MS, and Farese JP (2013) Melanoma, in *Small Animal Clinical Oncology*, 5th ed (Withrow S, Vail D, and Page R eds) pp 321–334, Elsevier, St. Louis, MO.
Bhaumik A, Shearin AM, Delong R, Wanekaya A, and Ghosh K (2014) Probing the interaction at the nano-bio interface using raman spectroscopy: ZnO nanoparticles and adenosine triphosphate biomolecules. *J Phys Chem C Nanomater Interfaces* **118**:18631–18639.
Bocanegra Gondan AI, Ruiz-de-Angulo A, Zabaleta A, Gómez Blanco N, Cobaleda-Siles BM, García-Granda MJ, Padro D, Llop J, Arnaiz B, Gato M, et al. (2018) Effective cancer immunotherapy in mice by polyIC-imiquimod complexes and engineered magnetic nanoparticles. *Biomaterials* **170**:95–115.
Bronson RT (1982) Variation in age at death of dogs of different sexes and breeds. *Am J Vet Res* **43**:2057–2059.
Cancer Genome Atlas Network (2015) Genomic classification of cutaneous melanoma. *Cell* **161**:1681–1696.
Canoa P, Simón-Vázquez R, Popplewell J, and González-Fernández Á (2015) A quantitative binding study of fibrinogen and human serum albumin to metal oxide nanoparticles by surface plasmon resonance. *Biosens Bioelectron* **74**:376–383.
Cao Y, Wang B, Wang Y, and Lou D (2014) Dual drug release from core-shell nanoparticles with distinct release profiles. *J Pharm Sci* **103**:3205–3216.
Carlander U, Li D, Jolliet O, Emond C, and Johanson G (2016) Toward a general physiologically-based pharmacokinetic model for intravenously injected nanoparticles. *Int J Nanomedicine* **11**:625–640.
Cha SH, Hong J, McGuffie M, Yeom B, VanEpps JS, and Kotov NA (2015) Shape-dependent biomimetic inhibition of enzyme by nanoparticles and their antibacterial activity. *ACS Nano* **9**:9097–9105.
Chang AE, Karnell LH, and Menck HR (1998) The National Cancer Data Base report on cutaneous and noncutaneous melanoma: a summary of 84,836 cases from the past decade. The American College of Surgeons Commission on Cancer and the American Cancer Society. *Cancer* **83**:1664–1678.
Chen WY, Cheng YH, Hsieh NH, Wu BC, Chou WC, Ho CC, Chen JK, Liao CM, and Lin P (2015) Physiologically based pharmacokinetic modeling of zinc oxide nanoparticles and zinc nitrate in mice. *Int J Nanomedicine* **10**:6277–6292.
Cheng X, DeLong RK, Wickstrom E, Kligshteyn M, Demirdji SH, Caruthers MH, and Juliano RL (1997) Interactions between single-stranded DNA binding protein and oligonucleotide analogs with different backbone chemistries. *J Mol Recognit* **10**:101–107.
Choi J, Kim H, Kim P, Jo E, Kim HM, Lee MY, Jin SM, and Park K (2015) Toxicity of zinc oxide nanoparticles in rats treated by two different routes: single intravenous injection and single oral administration. *J Toxicol Environ Health A* **78**:226–243.

Choi SJ and Choy JH (2014) Biokinetics of zinc oxide nanoparticles: toxicokinetics, biological fates, and protein interaction. *Int J Nanomedicine* **9** (**Suppl 2**):261–269.
Cobaleda-Siles M, Henriksen-Lacey M, Ruiz de Angulo A, Bernecker A, Gómez Vallejo V, Szczupak B, Llop J, Pastor G, Plaza-Garcia S, Jauregui-Osoro M, et al. (2014) An iron oxide nanocarrier for dsRNA to target lymph nodes and strongly activate cells of the immune system. *Small* **10**:5054–5067.
Curtin JA, Busam K, Pinkel D, and Bastian BC (2006) Somatic activation of KIT in distinct subtypes of melanoma. *J Clin Oncol* **24**:4340–4346.
Dai Q, Wilhelm S, Ding D, Syed AM, Sindhwani S, Zhang Y, Chen YY, MacMillan P, and Chan WCW (2018) Quantifying the ligand-coated nanoparticle delivery to cancer cells in solid tumors. *ACS Nano* **12**:8423–8435.
Danhier F, Feron O, and Préat V (2010) To exploit the tumor microenvironment: passive and active tumor targeting of nanocarriers for anti-cancer drug delivery. *J Control Release* **148**:135–146.
Davies H, Bignell GR, Cox C, Stephens P, Edkins S, Clegg S, Teague J, Woffendin H, Garnett MJ, Bottomley W, et al. (2002) Mutations of the BRAF gene in human cancer. *Nature* **417**:949–954.
DeLong RK, Akhtar U, Sallee M, Parker B, Barber S, Zhang J, Craig M, Garrad R, Hickey AJ, and Engstrom E (2009) Characterization and performance of nucleic acid nanoparticles combined with protamine and gold. *Biomaterials* **30**:6451–6459.
DeLong RK and Curtis CB (2017) Toward RNA nanoparticle vaccines: synergizing RNA and inorganic nanoparticles to achieve immunopotentiation. *Wiley Interdiscip Rev Nanomed Nanobiotechnol* **9**:e1415.
DeLong RK and Hurst M (2018) inventors, Kansas State University Research Foundation, Manhattan, KS (US), assignee. Two dimensional fluorescence difference spectroscopy characterization of nanoparticles and their interactions. U.S. patent 9,977,016. May 22, 2018.
DeLong RK, Mitchell JA, Morris RT, Comer J, Hurst MN, Ghosh K, Wanekaya A, Mudge M, Schaeffer A, Washington LL, et al. (2017) Enzyme and cancer cell selectivity of nanoparticles: inhibition of 3D metastatic phenotype and experimental melanoma by zinc oxide. *J Biomed Nanotechnol* **13**:221–231.
DeLong RK, Nolting A, Fisher M, Chen Q, Wickstrom E, Kligshteyn M, Demirdji S, Caruthers M, and Juliano RL (1997) Comparative pharmacokinetics, tissue distribution, and tumor accumulation of phosphorothioate, phosphorodithioate, and methylphosphonate oligonucleotides in nude mice. *Antisense Nucleic Acid Drug Dev* **7**:71–77.
Delong RK, Reynolds CM, Malcolm Y, Schaeffer A, Severs T, and Wanekaya A (2010) Functionalized gold nanoparticles for the binding, stabilization, and delivery of therapeutic DNA, RNA, and other biological macromolecules. *Nanotechnol Sci Appl* **3**:53–63.
Delong RK, Risor A, Kanomata M, Laymon A, Jones B, Zimmerman SD, Williams J, Witkowski C, Warner M, Ruff M, et al. (2012) Characterization of biomolecular nanoconjugates by high-throughput delivery and spectroscopic difference. *Nanomedicine (Lond)* **7**:1851–1862.
Du Y, Xia L, Jo A, Davis RM, Bissel P, Ehrich MF, and Kingston DGI (2018) Synthesis and evaluation of doxorubicin-loaded gold nanoparticles for tumor-targeted drug delivery. *Bioconjug Chem* **29**:420–430.
Felício MR, Silva ON, Gonçalves S, Santos NC, and Franco OL (2017) Peptides with dual antimicrobial and anticancer activities. *Front Chem* **5**:5.
Fowles JS, Denton CL, and Gustafson DL (2015) Comparative analysis of MAPK and PI3K/AKT pathway activation and inhibition in human and canine melanoma. *Vet Comp Oncol* **13**:288–304.
Fujihara J, Tongu M, Hashimoto H, Yamada T, Kimura-Kataoka K, Yasuda T, Fujita Y, and Takeshita H (2015) Distribution and toxicity evaluation of ZnO dispersion nanoparticles in single intravenously exposed mice. *J Med Invest* **62**:45–50.
Ganguly A, Trinh P, Ramanujachary KV, Ahmad T, Mugweru A, and Ganguli AK (2011) Reverse micellar based synthesis of ultrafine MgO nanoparticles (8–10 nm): characterization and catalytic properties. *J Colloid Interface Sci* **353**:137–142.
Gann H, Glaspell G, Garrad R, Wanekaya A, Ghosh K, Cillessen L, Scholz A, Parker B, Warner M, and Delong RK (2010) Interaction of MnO and ZnO nanomaterials with biomedically important proteins and cells. *J Biomed Nanotechnol* **6**:37–42.
Gopala Krishna P, Paduvarahalli Ananthaswamy P, Yadavalli T, Bhangi Mutta N, Sannaiah A, and Shivanna Y (2016) ZnO nanopellets have selective anticancer activity. *Mater Sci Eng C* **62**:919–926.
Gordon I, Paoloni M, Mazcko C, and Khanna C (2009) The Comparative Oncology Trials Consortium: using spontaneously occurring cancers in dogs to inform the cancer drug development pathway. *PLoS Med* **6**:e1000161.
Gordon IK and Khanna C (2010) Modeling opportunities in comparative oncology for drug development. *ILAR J* **51**:214–220.
Gragoudas ES, Adamis AP, Cunningham ET Jr, Feinsod M, and Guyer DR; VEGF Inhibition Study in Ocular Neovascularization Clinical Trial Group (2004) Pegaptanib for neovascular age-related macular degeneration. *N Engl J Med* **351**: 2805–2816.
Hanley C, Layne J, Punnoose A, Reddy KM, Coombs I, Coombs A, Feris K, and Wingett D (2008) Preferential killing of cancer cells and activated human T cells using ZnO nanoparticles. *Nanotechnology* **19**:295103.
Hansen K and Khanna C (2004) Spontaneous and genetically engineered animal models; use in preclinical cancer drug development. *Eur J Cancer* **40**:858–880.
Hendricks WPD, Zismann V, Sivaprakasam K, Legendre C, Poorman K, Tembe W, Perdigones N, Kiefer J, Liang W, DeLuca V, et al. (2018) Somatic inactivating *PTPRJ* mutations and dysregulated pathways identified in canine malignant melanoma by integrated comparative genomic analysis. *PLoS Genet* **14**:e1007589.
Hernandez B, Adissu HA, Wei BR, Michael HT, Merlino G, and Simpson RM (2018) Naturally occurring canine melanoma as a predictive comparative oncology model for human mucosal and other triple wild-type melanomas. *Int J Mol Sci* **19**:E394.
Hicks J, Platt S, Kent M, and Haley A (2017) Canine brain tumours: a model for the human disease? *Vet Comp Oncol* **15**:252–272.
Hong H, Wang F, Zhang Y, Graves SA, Eddine SB, Yang Y, Theuer CP, Nickles RJ, Wang X, and Cai W (2015) Red fluorescent zinc oxide nanoparticle: a novel platform for cancer targeting. *ACS Appl Mater Interfaces* **7**:3373–3381.
Hue JJ, Lee HJ, Nam SY, Kim JS, Lee BJ, and Yun YW (2015) Distribution and accumulation of ^{177}Lu-labeled thermally cross-linked superparamagnetic iron oxide nanoparticles in the tissues of ICR mice. *Korean J Vet Sci* **55**:57–60.
Hurst MN and DeLong RK (2016) Two-dimensional fluorescence difference spectroscopy to characterize nanoparticles and their interactions. *Sci Rep* **6**:33287.
Ito D, Frantz AM, and Modiano JF (2014) Canine lymphoma as a comparative model for human non-Hodgkin lymphoma: recent progress and applications. *Vet Immunol Immunopathol* **159**:192–201.
Jia J, Zheng Y, Wang W, Shao Y, Li Z, Wang Q, Wang Y, and Yan H (2017) Antimicrobial peptide LL-37 promotes YB-1 expression, and the viability, migration and invasion of malignant melanoma cells. *Mol Med Rep* **15**:240–248.
Kelleher FC and McArthur GA (2012) Targeting NRAS in melanoma. *Cancer J* **18**: 132–136.
Khanna C, London C, Vail D, Mazcko C, and Hirschfeld S (2009) Guiding the optimal translation of new cancer treatments from canine to human cancer patients. *Clin Cancer Res* **15**:5671–5677.
Kimoto M, Shirouzu M, Mizutani S, Koide H, Kaziro Y, Hirao I, and Yokoyama S (2002) Anti-(Raf-1) RNA aptamers that inhibit Ras-induced Raf-1 activation. *Eur J Biochem* **269**:697–704.
Kiuru M and Busam KJ (2017) The NF1 gene in tumor syndromes and melanoma. *Lab Invest* **97**:146–157.
Knapp DW, Ramos-Vara JA, Moore GE, Dhawan D, Bonney PL, and Young KE (2014) Urinary bladder cancer in dogs, a naturally occurring model for cancer biology and drug development. *ILAR J* **55**:100–118.
Kunz M (2014) Oncogenes in melanoma: an update. *Eur J Cell Biol* **93**:1–10.
Lankveld DP, Oomen AG, Krystek P, Neigh A, Troost-de Jong A, Noorlander CW, Van Eijkeren JC, Geertsma RE, and De Jong WH (2010) The kinetics of the tissue distribution of silver nanoparticles of different sizes. *Biomaterials* **31**:8350–8361.
LeBlanc AK, Mazcko CN, and Khanna C (2016) Defining the value of a comparative approach to cancer drug development. *Clin Cancer Res* **22**:2133–2138.
Lellouche E, Israel LL, Bechor M, Attal S, Kurlander E, Asher VA, Dolitzky A, Shaham L, Izraeli S, Lellouche JP, et al. (2015) MagRET nanoparticles: an iron oxide nanocomposite platform for gene silencing from microRNAs to long noncoding RNAs. *Bioconjug Chem* **26**:1692–1701.
Li CH, Shen CC, Cheng YW, Huang SH, Wu CC, Kao CC, Liao JW, and Kang JJ (2012) Organ biodistribution, clearance, and genotoxicity of orally administered zinc oxide nanoparticles in mice. *Nanotoxicology* **6**:746–756.
Li J, Wang Y, Liang R, An X, Wang K, Shen G, Tu Y, Zhu J, and Tao J (2015) Recent advances in targeted nanoparticles drug delivery to melanoma. *Nanomedicine (Lond)* **11**:769–794.
Li M, Al-Jamal KT, Kostarelos K, and Reineke J (2010) Physiologically based pharmacokinetic modeling of nanoparticles. *ACS Nano* **4**:6303–6317.
Li M, Zou P, Tyner K, and Lee S (2017) Physiologically based pharmacokinetic (PBPK) modeling of pharmaceutical nanoparticles. *AAPS J* **19**:26–42.
Lin YG, Hsu YK, Chen SY, Lin YK, Chen LC, and Chen KH (2009) Nanostructured zinc oxide nanorods with copper nanoparticles as a microreformation catalyst. *Angew Chem Int Ed Engl* **48**:7586–7590.
Lin Z, Monteiro-Riviere NA, Kannan R, and Riviere JE (2016a) A computational framework for interspecies pharmacokinetics, exposure and toxicity assessment of gold nanoparticles. *Nanomedicine (Lond)* **11**:107–119.
Lin Z, Monteiro-Riviere NA, and Riviere JE (2015) Pharmacokinetics of metallic nanoparticles. *Wiley Interdiscip Rev Nanomed Nanobiotechnol* **7**:189–217.
Lin Z, Monteiro-Riviere NA, and Riviere JE (2016b) A physiologically based pharmacokinetic model for polyethylene glycol-coated gold nanoparticles of different sizes in adult mice. *Nanotoxicology* **10**:162–172.
Liu Q, Das M, Liu Y, and Huang L (2018) Targeted drug delivery to melanoma. *Adv Drug Deliv Rev* **127**:208–221.
Manshian BB, Pokhrel S, Himmelreich U, Tämm K, Sikk L, Fernández A, Rallo R, Tamm T, Mädler L, and Soenen SJ (2017) In silico design of optimal dissolution kinetics of Fe-doped ZnO nanoparticles results in cancer-specific toxicity in a preclinical rodent model. *Adv Healthc Mater* **6**:1601379.
McCall J, Smith JJ, Marquardt KN, Knight KR, Bane H, Barber A, and DeLong RK (2017) ZnO nanoparticles protect RNA from degradation better than DNA. *Nanomaterials (Basel)* **7**:E378.
Mishra PK, Mishra H, Ekielski A, Talegaonkar S, and Vaidya B (2017) Zinc oxide nanoparticles: a promising nanomaterial for biomedical applications. *Drug Discov Today* **22**:1825–1834.
Moon SH, Choi WJ, Choi SW, Kim EH, Kim J, Lee JO, and Kim SH (2016) Anticancer activity of ZnO chips by sustained zinc ion release. *Toxicol Rep* **3**:430–438.
Nass SJ and Gorby H, editors (2015) *The Role of Clinical Studies for Pets with Naturally Occurring Tumors in Translational Cancer Research: Workshop Summary*, The National Academies Press, Washington, DC.
Nicolas J, Mura S, Brambilla D, Mackiewicz N, and Couvreur P (2013) Design, functionalization strategies and biomedical applications of targeted biodegradable/biocompatible polymer-based nanocarriers for drug delivery. *Chem Soc Rev* **42**:1147–1235.
Paek HJ, Lee YJ, Chung HE, Yoo NH, Lee JA, Kim MK, Lee JK, Jeong J, and Choi SJ (2013) Modulation of the pharmacokinetics of zinc oxide nanoparticles and their fates in vivo. *Nanoscale* **5**:11416–11427.
Paoloni MC and Khanna C (2007) Comparative oncology today. *Vet Clin North Am Small Anim Pract* **37**:1023–1032.
Paoloni M and Khanna C (2008) Translation of new cancer treatments from pet dogs to humans. *Nat Rev Cancer* **8**:147–156.
Pinho SS, Carvalho S, Cabral J, Reis CA, and Gärtner F (2012) Canine tumors: a spontaneous animal model of human carcinogenesis. *Transl Res* **159**:165–172.
Poon W, Zhang X, Bekah D, Teodoro JG, and Nadeau JL (2015) Targeting B16 tumors in vivo with peptide-conjugated gold nanoparticles. *Nanotechnology* **26**:285101.
Porrello A, Cardelli P, and Spugnini EP (2006) Oncology of companion animals as a model for humans. An overview of tumor histotypes. *J Exp Clin Cancer Res* **25**: 97–105.

Poulikakos PI, Persaud Y, Janakiraman M, Kong X, Ng C, Moriceau G, Shi H, Atefi M, Titz B, Gabay MT, et al. (2011) RAF inhibitor resistance is mediated by dimerization of aberrantly spliced BRAF(V600E). *Nature* **480**:387–390.
Ramani M, Mudge MC, Morris RT, Zhang Y, Warcholek SA, Hurst MN, Riviere JE, and DeLong RK (2017a) Zinc oxide nanoparticle-poly I:C RNA complexes: implication as therapeutics against experimental melanoma. *Mol Pharm* **14**:614–625.
Ramani M, Nguyen TDT, Aryal S, Ghosh KC, and DeLong RK (2017b) Elucidating the RNA nano–bio interface: mechanisms of anticancer poly I:C RNA and zinc oxide nanoparticle interaction. *J Phys Chem C* **121**:15702–15710.
Rasmussen JW, Martinez E, Louka P, and Wingett DG (2010) Zinc oxide nanoparticles for selective destruction of tumor cells and potential for drug delivery applications. *Expert Opin Drug Deliv* **7**:1063–1077.
Riviere JE (2009) Pharmacokinetics of nanomaterials: an overview of carbon nanotubes, fullerenes and quantum dots. *Wiley Interdiscip Rev Nanomed Nanobiotechnol* **1**:26–34.
Robert C, Karaszewska B, Schachter J, Rutkowski P, Mackiewicz A, Stroiakovski D, Lichinitser M, Dummer R, Grange F, Mortier L, et al. (2015) Improved overall survival in melanoma with combined dabrafenib and trametinib. *N Engl J Med* **372**:30–39.
Rosenblum D, Joshi N, Tao W, Karp JM, and Peer D (2018) Progress and challenges towards targeted delivery of cancer therapeutics. *Nat Commun* **9**:1410.
Rowell JL, McCarthy DO, and Alvarez CE (2011) Dog models of naturally occurring cancer. *Trends Mol Med* **17**:380–388.
Roy R, Kumar S, Verma AK, Sharma A, Chaudhari BP, Tripathi A, Das M, and Dwivedi PD (2014a) Zinc oxide nanoparticles provide an adjuvant effect to ovalbumin via a Th2 response in Balb/c mice. *Int Immunol* **26**:159–172.
Roy R, Singh SK, Chauhan LK, Das M, Tripathi A, and Dwivedi PD (2014b) Zinc oxide nanoparticles induce apoptosis by enhancement of autophagy via PI3K/Akt/mTOR inhibition. *Toxicol Lett* **227**:29–40.
Sakamuri D, Glitza IC, Betancourt Cuellar SL, Subbiah V, Fu S, Tsimberidou AM, Wheler JJ, Hong DS, Naing A, Falchook GS, et al. (2018) Phase I dose-escalation study of anti-CTLA-4 antibody ipilimumab and lenalidomide in patients with advanced cancers. *Mol Cancer Ther* **17**:671–676.
Salton M, Kasprzak WK, Voss T, Shapiro BA, Poulikakos PI, and Misteli T (2015) Inhibition of vemurafenib-resistant melanoma by interference with pre-mRNA splicing. *Nat Commun* **6**:7103.
Schiffman JD and Breen M (2015) Comparative oncology: what dogs and other species can teach us about humans with cancer. *Philos Trans R Soc Lond B Biol Sci* **370**:20140231.
Simpson RM, Bastian BC, Michael HT, Webster JD, Prasad ML, Conway CM, Prieto VM, Gary JM, Goldschmidt MH, Esplin DG, et al. (2014) Sporadic naturally occurring melanoma in dogs as a preclinical model for human melanoma. *Pigment Cell Melanoma Res* **27**:37–47.
Simpson S, Dunning MD, de Brot S, Grau-Roma L, Mongan NP, and Rutland CS (2017) Comparative review of human and canine osteosarcoma: morphology, epidemiology, prognosis, treatment and genetics. *Acta Vet Scand* **59**:71.
Singh D, Qi R, Jordan JL, San Mateo L, and Kao CC (2013) The human antimicrobial peptide LL-37, but not the mouse ortholog, mCRAMP, can stimulate signaling by poly(I:C) through a FPRL1-dependent pathway. *J Biol Chem* **288**:8258–8268.
Stein CA and Castanotto D (2017) FDA-approved oligonucleotide therapies in 2017. *Mol Ther* **25**:1069–1075.
Sulaimon SS and Kitchell BE (2003) The basic biology of malignant melanoma: molecular mechanisms of disease progression and comparative aspects. *J Vet Intern Med* **17**:760–772.
Sykes EA, Dai Q, Sarsons CD, Chen J, Rocheleau JV, Hwang DM, Zheng G, Cramb DT, Rinker KD, and Chan WC (2016) Tailoring nanoparticle designs to target cancer based on tumor pathophysiology. *Proc Natl Acad Sci USA* **113**:E1142–E1151.
Thomas SE, Comer J, Kim MJ, Marroquin S, Murthy V, Ramani M, Hopke TG, McCall J, Choi SO, and DeLong RK (2018) Comparative functional dynamics studies on the enzyme nano-bio interface. *Int J Nanomedicine* **13**:4523–4536.
Tran S, DeGiovanni PJ, Piel B, and Rai P (2017) Cancer nanomedicine: a review of recent success in drug delivery. *Clin Transl Med* **6**:44.
Wang C, Lu J, Zhou L, Li J, Xu J, Li W, Zhang L, Zhong X, and Wang T (2016) Effects of long-term exposure to zinc oxide nanoparticles on development, zinc metabolism and biodistribution of minerals (Zn, Fe, Cu, Mn) in mice. *PLoS One* **11**:e0164434.
Weber J, Mandala M, Del Vecchio M, Gogas HJ, Arance AM, Cowey CL, Dalle S, Schenker M, Chiarion-Sileni V, Marquez-Rodas I, et al.; CheckMate 238 Collaborators (2017) Adjuvant nivolumab versus ipilimumab in resected stage III or IV melanoma. *N Engl J Med* **377**:1824–1835.
Wilhelm S, Tavares AJ, Dai Q, Ohta S, Audet J, Dvorak HF, and Chan WCW (2016) Analysis of nanoparticle delivery to tumours. *Nat Rev Mater* **1**:16014.
Ye DX, Ma YY, Zhao W, Cao HM, Kong JL, Xiong HM, and Möhwald H (2016) ZnO-based nanoplatforms for labeling and treatment of mouse tumors without detectable toxic side effects. *ACS Nano* **10**:4294–4300.
Yeh TK, Chen JK, Lin CH, Yang MH, Yang CS, Chou FI, Peir JJ, Wang MY, Chang WH, Tsai MH, et al. (2012) Kinetics and tissue distribution of neutron-activated zinc oxide nanoparticles and zinc nitrate in mice: effects of size and particulate nature. *Nanotechnology* **23**:085102.
Yun JW, Yoon JH, Kang BC, Cho NH, Seok SH, Min SK, Min JH, Che JH, and Kim YK (2015) The toxicity and distribution of iron oxide-zinc oxide core-shell nanoparticles in C57BL/6 mice after repeated subcutaneous administration. *J Appl Toxicol* **35**:593–602.
Zhang H, Ji Z, Xia T, Meng H, Low-Kam C, Liu R, Pokhrel S, Lin S, Wang X, Liao YP, et al. (2012) Use of metal oxide nanoparticle band gap to develop a predictive paradigm for oxidative stress and acute pulmonary inflammation. *ACS Nano* **6**:4349–4368.
Zhang Z, Wan J, Sun L, Li Y, Guo J, and Wang C (2016) Zinc finger-inspired nanohydrogels with glutathione/pH triggered degradation based on coordination substitution for highly efficient delivery of anti-cancer drugs. *J Control Release* **225**:96–108.

Address correspondence to: R.K. DeLong, Department of Anatomy and Physiology, Nanotechnology Innovation Center, College of Veterinary Medicine, Kansas State University, 1800 Denison Avenue, Manhattan, KS 66506. E-mail: robertdelong@ksu.edu; or Mary Lynn Higginbotham, Department of Clinical Sciences, College of Veterinary Medicine, Kansas State University, 1800 Denison Avenue, Manhattan, KS 66506. E-mail: mhigginb@vet.k-state.edu